Wide Passband Design for Cosine-Modulated Filter Banks in Sinusoidal Speech Synthesis

Nobuyuki Nishizawa and Tomonori Yazaki

KDDI R&D Laboratories Inc., Japan

{no-nishizawa, yazaki}@kddilabs.jp

Abstract

A new filter design strategy to shorten the length of the filter is introduced for sinusoidal speech synthesis using cosine-modulated filter banks. Multiple sinusoidal waveforms for speech synthesis can be effectively synthesized by using pseudo-quadrature mirror filter (pseudo-QMF) banks, which are constructed by cosine modulation of the coefficients of a low-pass filter. This is because stable sinusoids are represented as sparse vectors on the subband domain of the pseudo-QMF banks and computation for the filter banks can be effectively performed with fast algorithms for discrete cosine transformation (DCT). However, the pseudo-QMF banks require relatively long filters to reduce noise caused by aliasing. In this study, a wider passband design with a perfect reconstruction (PR) QMF bank is introduced. The properties of experimentally designed filters indicated that the length of the filters can be reduced from 448 taps to 384 taps for 32-subband systems with less than -96dB errors where the computational cost for speech synthesis does not significantly increase.

Index Terms: statistical parametric speech synthesis, speech waveform generation, sinusoidal speech synthesis, cosine-modulated filter bank

1. Introduction

For embedded speech synthesizers based on statistical parametric speech synthesis (SPSS) [1, 2] such as HMM-based speech synthesis [3, 4], the computational cost of the waveform generation is often problematic. In waveform generation, mel-log spectrum approximation (MLSA) filters [5] or auto-regressive (AR) filters are often used in speech synthesizers based on mel-cepstrum or linear spectrum pairs (LSP), respectively. For this type of filter processing, the number of required multiply-add operations is proportional to the length of the filter, i.e. the analysis order of melcepstrum or LSP. Consequently, several million or tens of millions of multiply-add operations per second are necessary for waveform generation. Since the computational cost corresponds to the power consumption in practice, its reduction is especially important for devices powered by small batteries, such as wearable devices.

To reduce the computational cost of waveform generation, we have proposed a method based on sinusoidal speech synthesis with a filter bank [6, 7]. In the proposed method, although the periodic components of speech waveforms are synthesized by the summation of sinusoidal waveforms, similarly to sinusoidal modeling [8] or the harmonic part of the harmonic-plus-noise model (HNM) [9], all operations are performed on the subband domain of pseudo-quadrature mirror filter (QMF) banks [10, 11], rather than the waveform domain. Since sinusoids are represented as sparse vectors on a subband domain with a reduced sampling rate, the computational cost of amplitude scaling and summation of sinusoids in sinusoidal speech synthesis can be significantly reduced by the proposed method. Consequently, the total computational cost of waveform generation can be reduced even when the cost of composing the subbands is taken into account.

However, the pseudo-QMF banks require long filters to suppress noise from aliasing caused by down-sampling and up-sampling in the filter banks. In such systems, response delays are long and over-smoothing of synthetic sounds can be caused by lower temporal resolutions. Moreover, the accumulation of calculation errors can become significant. In this study, as an alternative, wide passband designs using perfect reconstruction (PR) QMF banks are examined for speech waveform generation with shorter filters, where three or more subbands overlap on the frequency.

The rest of the paper is organized as follows. First, cosine-modulated filter banks and sinusoidal speech waveform generation on the filter banks are introduced in Section 2. Section 3 explains perfect-reconstruction QMF banks as the basis of the proposed method. Section 4 presents a design algorithm and experiment for the proposed method. Finally, section 5 concludes the paper.

2. Sinusoidal speech waveform generation using a pseudo-QMF bank

2.1. Cosine-modulated filter bank and pseudo-QMF bank

Figure 1 schematically shows the structure of the subband coding system based on maximally-decimated filter banks, where M is the number of subbands. In the system, M samples are converted into an M-dimensional vector. The output of the filter bank is given by

$$Y(z) = \sum_{l=0}^{M-1} A_l(z) X(zW_M^l) \tag{1}$$

where

$$A_l(z) = \frac{1}{M} \sum_{k=0}^{M-1} F_k(z) H_k(zW_M^l) \tag{2}$$

$$W_M = e^{-j\frac{2\pi}{M}}. \tag{3}$$

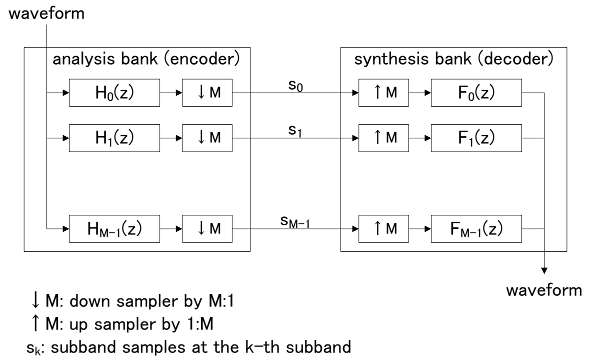

Figure 1: Block diagram of the subband coding system based on maximally-decimated filter banks.

For perfect reconstruction of the input signals, filter bank transfer and alias transfer functions $A_0(z)$ and $A_l(z)$ should be as follows:

$$A_0(z) = z^{-n_0} \quad (4)$$

$$A_l(z) = 0 \quad (1 \le l \le M-1), \quad (5)$$

respectively, where n_0 is the delay in samples [12].

For the cosine-modulated filter banks [12], $H_k(z)$ and $F_k(z)$ are given as follows:

$$H_k(z) = e^{j\theta_k} W_{2M}^{(k+1/2)\frac{N}{2}} H(zW_{2M}^{k+1/2}) + e^{-j\theta_k} W_{2M}^{-(k+1/2)\frac{N}{2}} H(zW_{2M}^{-(k+1/2)}) \quad (6)$$

$$F_k(z) = z^{-N} H_k(z^{-1}) \quad (7)$$

where

$$\theta_k = (-1)^k \pi/4 \quad (8)$$

and $H(z)$ is a low-pass filter, which is called a prototype filter. For $H(z)$, a linear-phase finite impulse response filter is often used. In such cases, the filter coefficients for $H_k(z)$ and $F_k(z)$ can be given by cosine modulation of the coefficients of the prototype filter $H(z)$.

The pseudo-QMF bank [10, 11] is a kind of cosine-modulated filter bank. In pseudo-QMF banks, although aliases between adjacent subbands caused by down-sampling and up-sampling should cancel each other, suppression of aliases between non-adjacent subbands (i.e. $A_l(z)$ for $l \ge 2$) is approximately achieved by stopband attenuation of $H_k(z)$ and $F_k(z)$, where the stopband edge angular frequency ω_s of the prototype filter must be equal to or less than π/M. The pseudo-QMF banks are used in subband coding such as MPEG Audio [13], where 32-band filter banks are used in which the length of the filters is 512 taps. Figure 2 shows plots of the coefficients and the frequency-vs-magnitude response of the prototype filter from the MPEG audio specification. Figure 3 shows the frequency-vs-magnitude responses of the cosine modulated filters for the analysis bank.

In practice, processing for the cosine-modulated filter bank can be performed with discrete cosine transformation (DCT). For fast processing, DCT corresponding to the cosine-modulation is performed at runtime with fast DCT algorithms [14, 15]. For example, a 32-point DCT processed by the algorithm proposed in [15] requires 80 multiplications and 209

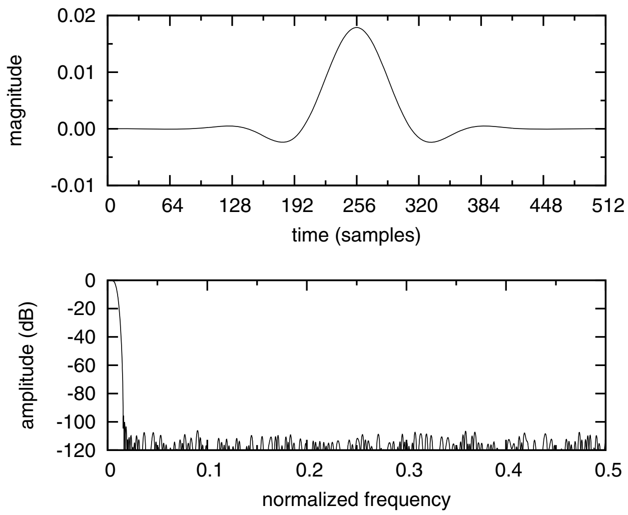

Figure 2: Impulse response and frequency-vs-amplitude response of the prototype filter for a 32-band pseudo-QMF bank.

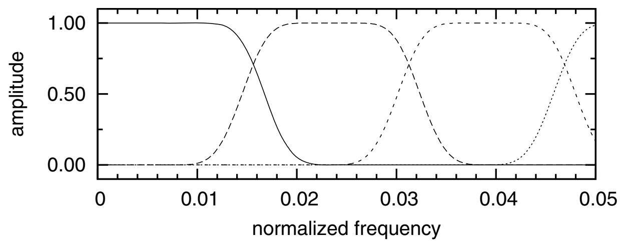

Figure 3: Frequency-vs-amplitude response of the filters for 0th (lowest) to 3rd bands in the analysis bank for $M = 32$ where amplitude plots in a linear scale.

additions. For the subband synthesis corresponding to the right half of Figure 1, DCT is performed for each subband vector first, and then, they are concatenated as a sequence [16]. Finally, the coefficients of the prototype filter and the elements of the sequence are multiplied. This means one M-point DCT operation and $N+1$ multiplications are needed for each vector of the subband (i.e. M samples in the output) in the subband composition based on the cosine-modulated filter banks, where $N+1$ is the length of the filter.

2.2. Sinusoidal speech synthesis with pseudo-QMF banks [6, 7]

A stable sinusoidal waveform can be encoded into a sparse vector by $H_k(z)$ with a reduced sampling rate by using the pseudo-QMF banks since the sinusoid becomes a line spectrum in the frequency domain. Consequently, each vector for a sinusoid has only two non-zero elements. In other words, the number of samples needed to represent a sinusoid is reduced to $2/M$ times with the pseudo-QMF bank. Moreover, the vectors for sinusoids can be computed directly [6]. This means that only the synthesis bank of the pseudo-QMF bank corresponding to the right-hand part of Figure 1 is necessary for a sinusoidal speech synthesizer.

For sinusoidal speech synthesis, a formulation is introduced in which waveforms are built by summation of cosine functions:

$$x(t) = \sum_j R(t, j \times \omega_0(t)) \cos(j \times \omega_0(t) \times (t - t_0)) \quad (9)$$

where $\omega_0(t)$, j, $R(t, \omega)$ and t_0 are the angular frequency of the fundamental vibration at time t, a positive integer as j of the j-th harmonic component, amplitude of the target sound at ω at time t and the position of the corresponding impulse, respectively. In this study, it is assumed that $\omega_0(t)$ and $R(t, \omega)$ are determined by HMM-based speech synthesis techniques from target texts of speech synthesis, where $R(t, \omega)$ can be calculated from the melcepstrum used in the conventional HMM-based speech synthesis systems.

Since operations for the synthesis bank of the cosine-modulated filter bank consist only of linear operations, the summation in Eq. (9) can be performed by the summation of the vectors into which sinusoids are encoded. The k-th element of the vector for a cosine waveform with angular frequency ω_j is given as follows:

$$s_{k,\omega_j}(t) = H_k(\omega_j) R(t, \omega_j) \cos(\omega_j(t - t_0) + \theta_k) \quad (10)$$

where $H_k(\omega)$ is the frequency-vs-magnitude response function of the filter for the k-th subband. Since $s_{k,\omega_j}(t)$ approximately equals zero at the stopband of $H_k(\omega_j)$, the computational cost of the summation of sinusoids can be drastically reduced by operating in the subband domain.

In practice, reduction of the calculation cost for $H_k(\omega)$ and $R(t, \omega)$ is critical. This can easily be achieved by using a pre-calculated table for $H_k(\omega)$ and fast DCT for $R(t, \omega)$, respectively, with linear interpolation [7].

3. Wide passband design with perfect-reconstruction QMF banks

As mentioned in Section 2.1, both $\omega_s \leq \pi/M$ and higher attenuation of the stopband of the filters must be simultaneously satisfied for the pseudo-QMF banks. Consequently, long filters are required to represent the steep slopes in the passband of the filters. In this study, a configuration in which $\omega_s > \pi/M$ is examined as an alternative. Since this makes the slope of the filter *gentle*, adequate stopband attenuation for speech waveform generation may be achieved with shorter filters.

However, when $\omega_s > \pi/M$, alias components between non-adjacent subband pairs must also be taken into account since some aliasing components caused by up-sampling pass through the passbands of the filters. Consequently, design algorithms for perfect reconstruction (PR) QMF banks [17] are used instead in this study. These are also a kind of cosine-modulated filter bank.

Referring to [17], PR-QMF banks can be achieved when the length of the prototype filter N is $2KM - 1$ where K is an integer, and

$$\sum_{r=0}^{2K-2k-1} h(n + rM) h(n + rM + 2kM) = \frac{\delta(k)}{2M} \quad (11)$$

for $0 \leq n \leq M/2 - 1$ and $0 \leq k \leq K - 1$, where $h(n)$ is the impulse response of the prototype filter, and $\delta(0) = 1$ and $\delta(k) = 0$ for $k \neq 0$. Note that the above equation is actually satisfied for $0 \leq n \leq M - 1$ due to the symmetric structure of the impulse response of linear-phase filters.

In study [18], minimization of

$$e_s + \gamma e_d \quad (12)$$

is proposed for the design of the PR-QMF banks where e_s and e_d correspond to the stopband attenuation of the prototype filter and the distortion against Eq. (11), respectively, and are given as follows:

$$e_s = \frac{1}{\pi - \omega_s} \int_{\omega_s}^{\pi} |H(e^{j\omega})|^2 d\omega \quad (13)$$

$$e_d = \sum_{k=0}^{K-1} \sum_{n=0}^{M/2-1} \left(\sum_{r=0}^{2m-2k-1} h(n + rM) h(n + rM + 2kM) - \frac{\delta(k)}{2M} \right)^2 . \quad (14)$$

The balance between the stopband attenuation of the prototype filter and the distortion of the filter bank is controlled by parameter γ.

4. Experimental design of wide passband filters for cosine-modulated filter banks

4.1. Filter design algorithm

In this study, the algorithm based on the iterative least squares (ILS) method proposed in [18] was basically used to design filters. In the original method, e_s is approximated by:

$$e_s \simeq \frac{1}{L} \sum_n |H(e^{j\omega_n})|^2 = \frac{1}{L} p^T C^T C p \quad (15)$$

where

$$C_{i,j} = \cos(\omega_i j + 1/2) \quad (16)$$

$$p = (h(\frac{N+1}{2}), ..., h(N-1))^T \quad (17)$$

$$\omega_i = \omega_s + (\pi - \omega_s) \frac{i}{L-1}. \quad (18)$$

Parameter L controls fineness when calculating the stopband characteristics. However, larger L values can make the optimization less accurate due to difficulty in computation. In this study, L was set to $4 \times (N+1)$ based on preliminary evaluation.

Referring to Eqs. (13) and (14), the optimization proposed in [18] is based on minimizing the least square errors. However, minimization of the maximal value in $|e_s|$ can be more practical where the stopband attenuation in the worst case is optimized. Therefore, the iterative reweighted least square (IRLS) method proposed in [19] was also applied to determine e_s in this study. In the optimization, e_s in formula (12) was replaced by $\tilde{e}_s$:

$$\tilde{e}_s(i) \simeq \frac{1}{L} \sum_n |w_i(\omega_n) H(e^{j\omega_n})|^2 = \frac{1}{L} p^T C^T W_i^T W_i C p \quad (19)$$

where

$$W_i = \mathrm{diag}(w_i(\omega_0), ..., w_i(\omega_{L-1})) \quad (20)$$

$$w^*_{i+1}(\omega_n) = \begin{cases} w_i(\omega_n)(H_i(|e^{j\omega_n})|/g_{\max})^{\phi/2} \\ \qquad (|H_i(e^{j\omega_n})| > g_{\max}) \\ w_i(\omega_n) \quad (|H_i(e^{j\omega_n})| \leq g_{\max}) \end{cases} \quad (21)$$

$$w_{i+1}(\omega_n) = \frac{w^*_{i+1}(\omega_n)}{\sqrt{\frac{1}{L}(\sum_{n=0}^{L-1}(w^*_{i+1}(\omega_n))^2}} \quad (22)$$

and $H_i(z)$ and $w_i(\omega_n)$ are the estimates of $H(z)$ and the normalized weight of $\tilde{e}_s$ at the i-th iteration of the IRLS method, and $\phi = 0.5$ in this study. By this algorithm, the maximal error of $|e_s|$ converges on $g_{\max}$. The initial weight $w_0(\omega_n)$ was set to 1 for all ω_n.

4.2. Experimental design of filters

To study the feasibility of the proposed filter design, prototype filters with wide passbands for the proposed method were experimentally designed by the algorithm described in Section 4.1. In this study, the number of subbands M was fixed at 32, which was also the number used in our earlier studies and in MPEG Audio. The length of the filter was set to 192, 256, 320 or 384 since filter length $N + 1$ must be equal to nM for PR-QMF, where n is an integer. However, the stopband edge angular frequency ω_s of the prototype filter was targeted to $1.5\pi/M$ or $2\pi/M$, where 3 or 4 adjacent subbands overlap each other, respectively.

In the optimization of the filter parameters, both the maximum of the stopband attenuation and the alias transfer functions (i.e. $\max|e_s|$ and $\max|A_l(z)|$ for $l \geq 1$) were minimized simultaneously. However, the parameters γ and $g_{\max}$ in the optimization do not directly minimize $\max|e_s|$ and $\max|A_l(z)|$. Consequently, several configurations for γ and $g_{\max}$ were experimentally examined first, and then the optimal results were picked up where $\max|e_s|$ and all $\max|A_l(z)|$ were equally weighted. By contrast, $A_0(z)$ was not taken into account in the optimization.

Table 1 shows the results of this optimization. In the table, bold numbers mean the maximal errors through $\max|e_s|$ and $\max|A_l(z)|$. For comparison, Table 2 shows the properties of the prototype filters for pseudo-QMF banks that were designed by the IRLS algorithm proposed in [19]. Comparing Tables 1 and 2, the proposed method reduces errors. In other words, a shorter filter can be achieved by the proposed method. For example, comparing the forth row in Table 1 and the fifth row in Table 2 shows that errors of less than -96 dB can be achieved with filters 64-tap shorter than in the conventional method. By contrast, the differences in errors between $1.5\pi/M$ and $2\pi/M$ in ω_s were not significant in most cases. The conditions for perfect reconstruction may negate the effect of the wide passband design with $\omega_s \geq 2\pi/M$, where four or more band-passed components interfere each other.

Figure 4 illustrates an example where M=32, ω_s=$1.5\pi/M$ and N+1=384 for the proposed method and M=32, ω_s=π/M and N+1=448 for the conventional method using a QMF bank. The figure shows that a gentler characteristic is designed by the proposed method.

Table 1: Properties of experimentally designed prototype filters for the proposed method.

ω_s/π	N+1	$\max|A_0|$ [dB]	$\max|e_s|$ [dB]	$\max|A_1|$ [dB]	$\max|A_2|$ [dB]
1.5/32	192	5.97E-4	-58.9	**-58.5**	-70.41
1.5/32	256	2.03E-3	-76.5	**-73.0**	-109.5
1.5/32	320	1.41E-3	**-80.5**	-80.5	-90.3
1.5/32	384	4.92E-5	-97.4	**-96.3**	-133.1
2/32	192	2.42E-3	**-57.4**	-57.8	-69.7
2/32	256	2.04E-3	-75.3	**-73.6**	-104.37
2/32	320	3.32E-4	**-85.7**	-85.8	-104.7
2/32	384	5.54E-5	**-95.7**	-97.4	-122.9

Table 2: Properties of experimentally designed prototype filters for pseudo-QMF banks.

ω_s/π	N+1	$\max|A_0|$ [dB]	$\max|e_s|$ [dB]	$\max|A_1|$ [dB]	$\max|A_2|$ [dB]
1/32	192	3.66	-58.6	-60.5	**-53.1**
1/32	256	7.77E-1	-71.8	**-67.3**	-73.9
1/32	320	1.36E-1	-76.9	**-75.2**	-77.9
1/32	384	9.37E-2	-92.8	-89.9	**-84.0**
1/32	448	5.31E-3	-103.0	**-96.2**	-111.4

4.3. Discussion of computational costs

The computational complexities of the components of the proposed method are $O(N)$, $O(\log M)$ and $O(\omega_s J/M)$ for the filtering, DCT and sinusoid generation, respectively, where $N+1$, ω_s, M and J are the length and the stopband edge angular frequency of the prototype filter, the number of subbands and the number of sinusoids, respectively. In this discussion, M is a given constant ($M = 32$) because M corresponds to temporal resolution of the waveform generation, i.e., it significantly affects quality of speech sounds.

In practice, the computational costs for the filtering and sinusoid generation can be comparable. In many low-cost or low-power processors for embedded systems, the computational cost of multiplication often dominates that of addition or bit-shift operations. Therefore, we focus on the costs of multiplication. As described in Section 2.1, 64 multiplications are reduced by using a 64-tap-shorter filter. However, calculation of three adjacent elements for each vector on the subband domain is necessary where ω_s=$1.5\pi/M$.

In Eq. (10), calculation of $H_k(\omega)$ in the passband requires two multiplications for linear interpolation when a precalculated table for $H_k(\omega)$ is used. By contrast, no supplemental calculation is practically necessary for

$$R(t, \omega_j)\cos(\omega_j(t - t_0) + \theta_k) \quad (23)$$

in Eq. (10) because of the symmetry of the cosine function with θ_k, where only θ_k depends on subband k. Therefore, one multiplication with $H_k(\omega)$ is an additional necessity for an additional calculation for $s_{k,\omega_j}(t)$. Consequently, compared with the cost of the conventional method using a pseudo-QMF bank, three additional multiplications are needed per sinusoid where ω_s=$1.5\pi/M$.

For example, when the fundamental frequency is 187.5 Hz on 8 kHz-sampling systems where periodic speech waveforms

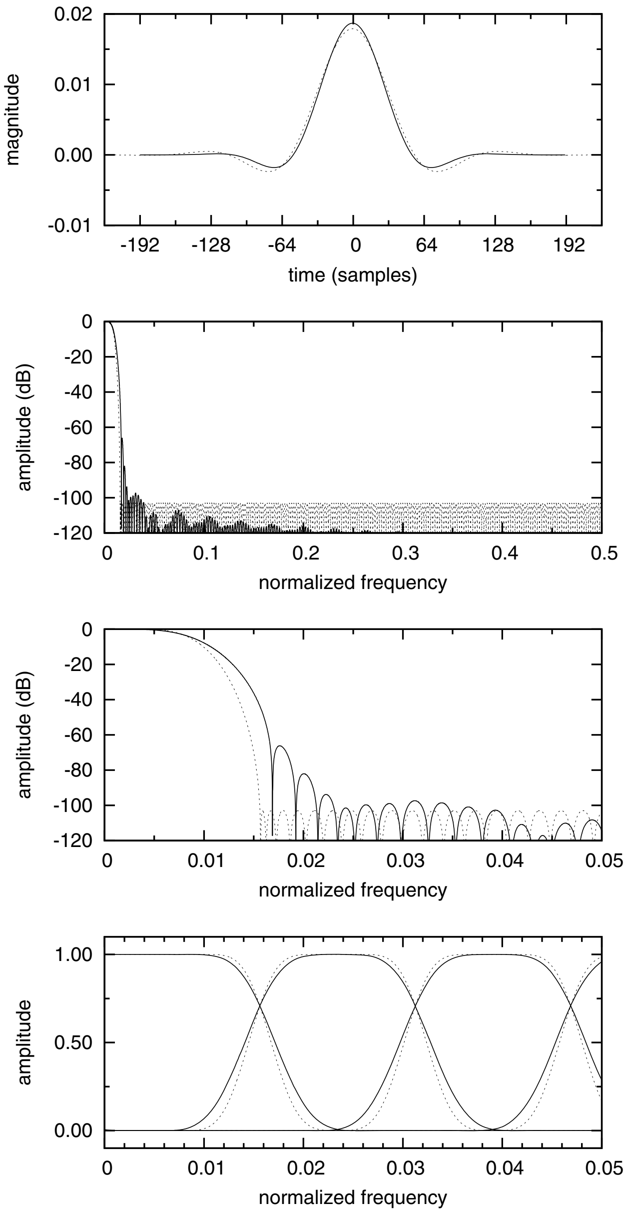

Figure 4: Impulse response, frequency-vs-amplitude responses of the prototype filter, and overlap structure of the proposed filter (solid line, M=32, ω_s=$1.5\pi/M$, N+1=384) and filter for pseudo-QMF bank (dotted line, M=32, ω_s=π/M and N+1=448).

are synthesized from 21.3 (=64/3) sinusoids, the computational cost of the vectors alone is comparable to that in the conventional methods. Although this frequency seems too high as the average fundamental frequency, the computational cost in practice is less than estimated since no operation for sinusoids is necessary for completely aperiodic speech sounds such as unvoiced phonemes and silence [7]. For example, where 30% of speech duration is unvoiced sound or silence, and the average fundamental frequency is higher than 131.3 Hz, the computational cost is reduced overall, relative to the cost of the conventional method. Thus, the total computational cost of the proposed method can be comparable to, or less than, that of the conventional method with a pseudo-QMF bank, at least where ω_s=$1.5\pi/M$. This means that the proposed method is applicable to sinusoidal speech waveform generation.

5. Conclusion

This paper has presented a wide passband design strategy for filters of the cosine-modulated filter banks used in sinusoidal speech synthesis. The properties of experimentally designed filters indicate that practical wide passband designs are possible where the passband width is 1.5 times as wide as that of the conventional pseudo-QMF banks. For example, the length of the filters can be reduced from 448 taps to 384 taps for 32-subband systems with less than -96 dB error. In that case, the proposed method does not significantly increase the computational cost.

In future work, reduction of the attenuation of the alias transfer functions as a more practical condition will be examined for shorter filters.

6. References

[1] Zen, H., Tokuda, K. and Black, A. W., “Statistical parametric speech synthesis,” Speech Communication, vol. 51(11), pp. 1039–1064, Nov. 2009.

[2] Tokuda, K., Nankaku, Y., Toda, T., Zen, H., Yamagishi, J. and Oura, K., “Speech synthesis based on hidden markov models,” Proc. of IEEE, vol. 101(5), pp. 1234-1252, May 2013.

[3] Masuko, T., Tokuda, K., Kobayashi, T. and Imai, S., “Speech synthesis using HMMs with dynamic features,” in Proc. of ICASSP ’96, vol. 1, pp. 389–392, May 1996.

[4] Yoshimura, T., Tokuda, K., Masuko, T., Kobayashi, T. and Kitamura, T., “Simultaneous modeling of spectrum, pitch and duration in HMM-based speech synthesis,” in Proc. Eurospeech ’99, pp. 2347–2350, Sep. 1999.

[5] Imai, S., “Cepstral analysis synthesis on the mel frequency scale,” in Proc. ICASSP ’83, vol. 8, pp. 93–96, Apr. 1983.

[6] Nishizawa, N. and Kato, T., “Speech synthesis using subband-coded multiband source components and sinusoids,” in Proc. ICASSP 2013, Vancouver, Canada, pp. 8002–8006, May. 2013.

[7] Nishizawa, N. and Kato, T., “Speech synthesis using a maximally decimated pseudo QMF bank for embedded devices,” in Proc. 8th ISCA Speech Synthesis Workshop, pp. 47–52, Aug. 2013.

[8] Quatieri, T. F. and McAulay, R. J., “Speech transformations based on a sinusoidal representation,” IEEE Trans. on ASSP, vol. 34(6), pp. 1449–1464, Dec. 1986.

[9] Stylianou, Y., Laroche, J. and Moulines, E. “High-quality speech modification based on a harmonic + noise model,” in Proc. Eurospeech, pp. 415-454, Sep. 1995,

[10] Rothweiler, J. H., “Polyphase quadrature filters – A new subband coding technique,” in Proc. ICASSP ’83, Boston, MA, U.S.A., vol. 3, pp. 1280–1283, Apr., 1983.

[11] Princen, J. P., Johnson, A. W. and Bradley, A. B., "Subband/transform coding using filter bank designs based on time domain aliasing cancellation," in Proc. ICASSP '87, Dallas, TX, U.S.A., vol. 4, pp. 2161–2164, Apr. 1987.

[12] Vaidyanathan, P. P., "Multirate Systems And Filter Banks," Prentice Hall, 1992.

[13] ISO/IEC, JTC1/SC29/WG11 MPEG, "Information technology – Coding of moving pictures and associated audio for digital storage media at up to about 1.5 Mbit/s Part 3: Audio," IS11172-3, 1992.

[14] Chen, W. H., Smith, C. H, and Fralick, S. C, "A fast computational algorithm for the discrete cosine transform," IEEE Trans. on Comm., vol. 25(9), pp. 1004–1009, Sep. 1977.

[15] Vetterli, M. and Nussbaumer, H. J., "Simple FFT and DCT algorithms with reduced number of operations," Signal Processing, vol. 6(4), pp. 267–278, Aug. 1984.

[16] Konstantinides, K., "Fast subband filtering in MPEG audio coding," IEEE SP Letters, vol. 1(2), pp 22–28, Feb. 1994.

[17] Malvar, H. S., "Modulated QMF filter banks with perfect reconstruction," Electronics Letters, vol. 26, no. 13, pp. 906-907, June 1990.

[18] Rossi, M., Zhang, J. Y. and Steenaart, W., "Iterative least squares design of perfect reconstruction QMF banks. ," in Proc. CCECE '96, Calgary, Alta., Canada, vol. 2, pp. 762–765, May 1996.

[19] Rossi, M., Zhang, J. Y. and Steenaart, W., "Iterative Constrained Least Squares Design of Near Perfect Reconstruction QMF Banks," in Proc. CCECE '96, Calgary, Alta., Canada, vol. 2, pp. 766–769, May 1996.